Author Manuscript

ORIGINAL ARTICLE

Small

Mixed-Transducer Micro-Origami for E cient Motion and Decoupled Sensing

Yi Zhu[1] | Anan Ghrayeb[1] | Joonyoung Yu[1] | Yiwei Yang[1] | Evgueni T. Filipov[1,2] | Kenn R. Oldham[1]

[1]Department of Mechanical Engineering, University of Michigan, Ann Arbor, MI, USA

[2]Department of Civil and Environmental Engineering, University of Michigan, Ann Arbor, MI, USA

Correspondence
Yi Zhu PhD, Department of Mechanical Engineering, University of Michigan, Ann Arbor, MI, 48109, USA
Email: yizhucee@umich.edu

Funding information
Defense Advanced Research Project Agency (DARPA) Grant D18AP00071; the National Science Foundation (NSF) Grant #2054148. The paper re ects the views and opinions of the authors, and not necessarily those of the funding entities.

This work introduces a mixed-transducer micro-origami to achieve ef cient vibration, controllable motion, and decoupled sensing. Existing micro-origami systems tend to have only one type of transducer (actuator/sensor), which limits their versatility and functionality because any given transducer system has a narrow range of advantageous working conditions. However, it is possible to harness the bene t of di erent micro-transducer systems to enhance the performance of functional micro-origami. More speci cally, this work introduces a micro-origami system that can integrate the advantages of three transducer systems: strained morph (SM) systems, polymer based electro-thermal (ET) systems, and thin- lm lead zirconate titanate (PZT) systems. A versatile photolithography fabrication process is introduced to build this mixed-transducer micro-origami system, and their performance is investigated through experiments and simulation models. This work shows that mixed-transducer micro-origami can achieve power e cient vibration with high frequency, large vibration ranges, and little degradation; can produce decoupled folding motion with good controllability; and can accomplish simultaneous sensing and actuation to detect and interact with external environments and small-scale samples. The superior performance of mixed-transducer micro-origami systems makes them promising tools for micro-manipulation, micro-assembly, biomedical probes, self-sensing metamaterials, and more.

KEYWORDS
micro-origami, strained morph, electro-thermal actuator, lead zirconate titanate, microelectromechanical systems

This is the author manuscript accepted for publication and has undergone full peer review but has not been through the copyediting, typesetting, pagination and proofreading process, which may lead to differences between this version and the Version of Record. Please cite this article as doi: 10.1002/smll.202400059

This article is protected by copyright. All rights reserved.

1 | INTRODUCTION

Microelectromechanical Systems (MEMS) and active structures provide useful tools for manipulating cells [1, 2, 3, 4, 5], executing minimally-invasive surgery [6, 7, 8], assembling metamaterials [9, 10], building micro-mirrors [11, 12], developing radio frequency switches [13, 14], building micro-robots [15, 16, 17, 18, 19], designing engineered fabrics [20, 21, 22, 23] and many more. Recently, the emergence of micro-origami systems has greatly enhanced the capabilities of existing MEMS devices because these micro-origami can fold into complex 3D geometries for sophisticated shape morphing and advanced functionality [24, 25, 26, 27, 28]. However, existing micro-origami and micro-robotic systems tend to rely on one onboard transducer system, which limits their motion complexity and sensing capability [24, 25, 26, 27, 28]. In this work, we demonstrate a mixed-transducer micro-origami system with enhanced ability to achieve e cient vibration, controllable motion, and decoupled sensing.

Figure 1A summarizes common transducer systems (for actuators or sensors) that can be used for building micro-origami and their folding performance. As can be seen, di erent transducer systems produce di erent performance. For example, surface electro-chemical actuators (green shade) can achieve small folding radius (good folding capability) but su ers from material degradation [27, 29]. Piezoelectric actuators can produce large output forces, have small power input, and have limited degradation, but have large folding radius (bad folding capability) [12, 30]. A more detailed summary of available transducer systems can be found in the Supplementary Text Section S1 and Table S1. Interested readers are referred to [31] for a thorough review on thin- lm actuators and [32] for active materials for functional origami at di erent length scales.

In general, each transducer system has its inherent bene ts and drawbacks. Therefore, it is bene cial to build micro-origami with mixed transducer systems to harness their advantageous properties and overcome their limitations. Moreover, integrating multiple transducers within a micro-origami can enable better motion control and sensing capability, because di erent transducers are decoupled in the electrical domain. However, integrating multiple transduction materials at micro-scale is challenging, because it requires developing appropriate micro-fabrication processes. Here, we overcome the limitations through developing a robust system design and a versatile photolithography based micro-fabrication process to organically integrate three di erent transducer systems. We focus on three micro-transducers: strained morph (SM) systems, electro-thermal (ET) systems, and thin- lm lead zirconate titanate (PZT) systems. Through experiments, we demonstrate that the fabricated mixed-transducer micro-origami can achieve power e cient and durable vibration, controllable and versatile motion, and decoupled sensing capability that are not possible with micro-origami or other MEMS devices using a single transduction mechanism.

Use of strained morphs (SM) is a common method for achieving self-assembly at the micro-scale. This actuation mechanism uses a bi-layer membrane to achieve a one-time folding motion [33, 34]. In most cases, one layer in the membrane develops a high residual stress during the fabrication process, and the residual stress will generate a large strain mismatch between the two layers inside the membrane. To reduce the strain mismatch and obtain equilibrium after release, the membrane will develop a curvature and fold to an angle. Using the strained morphs (SM) is bene cial because it requires no power input and can achieve a large folding angle [35, 36]. However, once released, the folding motion of the strained morph cannot be actively controlled.

Electro-thermal (ET) actuation is a popular transduction mechanism that can produce large folding motions actively [3, 4, 37, 18]. Past research has shown that these systems are useful for building micro cages [3, 4], micro-manipulators [38], and micro-grippers [24]. Among ET actuators, polymer-based systems can provide superior folding capabilities because of the high thermal-expansion coe cient of polymeric materials [24]. These polymer-based ET actuators can achieve relatively fast (10-100 Hz) active folding with large folding angle (>90°) and are durable. Prior work has shown that these ET systems can vibrate for more than around 100,000 cycles with no obvious degradation

Author Manuscript

This article is protected by copyright. All rights reserved.

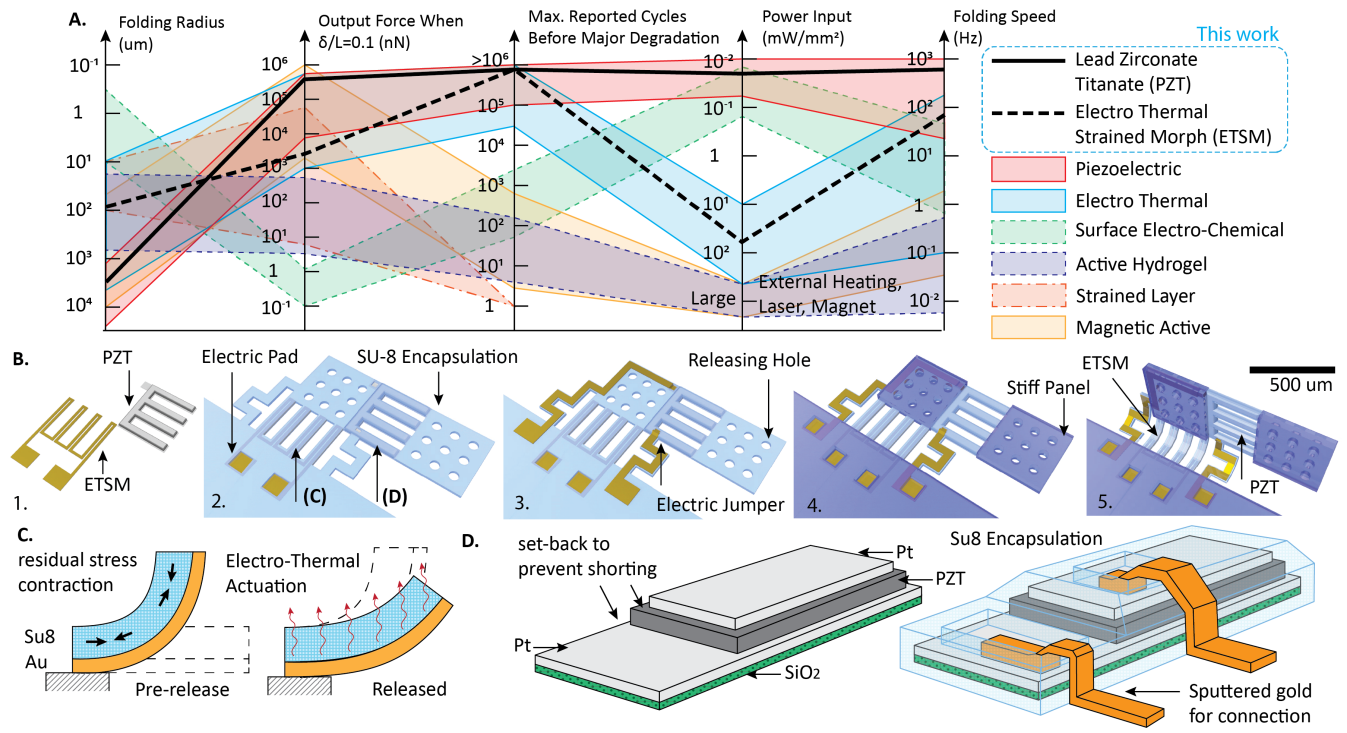


FIGURE 1 **Mixed-transducer micro-origami can harness bene□ts from di□erent transducer systems. A.** Reported performance of di□erent micro-transducer systems (reviewed in detail in Supplementary Text Section S1 and Table S1). Dashed boundary indicates function in aqueous environment. Solid boundary indicates function in atmospheric environment. Dash-dotted boundary indicates functioning in both. **B.** Fabrication process to combine strained morph (SM) transducer, electro-thermal (ET) transducer, and thin-□lm lead zirconate titanate (PZT) transducer within micro-origami. The strained morph (SM) can achieve 3D self-assembly with no power input; the electro-thermal (ET) transducer can achieve large active folding and piezoresistive sensing; and the thin-□lm lead zirconate titanate (PZT) transducer can achieve high-frequency and power e□ cient vibration. Figures are not drawn to scale for the thickness, the connection pads, and the releasing holes. **C.** Design of the electro-thermal strained morph (ETSM) system. **D.** Design of lead zirconate titanate (PZT) transducer.

[24]. In addition, these ET actuators can be used as strain gauges for sensing because these two systems have the same elements - ET heater wires can also serve as the structure of piezoresistive sensors. However, these ET systems require large power input to function and su□ers from limited controllability due to thermal coupling.

Thin-□lm lead zirconate titanate (PZT) is a piezoelectric ceramic material that can convert electrical charge to mechanical strain or vice versa with high conversion e□ ciency and high frequency (>1000 Hz) [39, 40]. PZT actuators are highly durable because piezoelectric actuation involves no chemical reaction. One example, presented later in this work shows that the PZT actuators can maintain vibration after 30 million cycles with no obvious degradation. Furthermore, because PZT is a metallic material, it has large Young's modulus and can produce larger output forces. These advantageous properties make PZT a good option for building micro-mirrors [41], micro-resonators [42, 43], and micro-scale legged-robots [12]. However, like other piezoelectric materials, PZT produces small actuation strain with limited range of motion. Because of the limited shape morphing capability, PZT systems cannot achieve 3D assembly on their own.

The paper is organized as follows. Section 2.1 discusses the design and folding capability of the mixed-transducer micro-origami system. Our design □rst combines the electro-thermal (ET) actuator and the strained morph (SM) system into one bi-material electro-thermal strained morph (ETSM) transducer. Next, a photolithographic micro-fabrication

Author Manuscript

This article is protected by copyright. All rights reserved.

method is introduced to fabricate the ETSM transducer and the PZT system for functional mixed-transducer micro-origami, and the performance characteristics of both systems are investigated using simulations and experiments. Following the design and fabrication, section 2.2 to section 2.4 show that our mixed-transducer micro-origami systems can achieve functionality beyond micro-systems relying on a single transducers. Section 2.2 shows that our micro-origami can achieve e cient vibrations with large motion range (>45°), high frequency (>100 Hz), and exceptional durability (no obvious degradation after 30 million cycles). Section 2.3 shows that mixed-transducers micro-origami can avoid coupling for controllable motions - folding an ETSM crease can generate motions in adjacent ETSM creases due to thermal coupling, but will not generate motions in adjacent PZT creases. Section 2.4, shows that mixed-transducer micro-origami can achieve decoupled sensing while maintaining actuation. Our experiments show that these micro-origami systems can acquire clean sensing signals through the ETSM transducers while actively interacting with external objects using the PZT actuators. Finally, we end the paper with a brief discussion on potential applications and future research directions. We believe the capabilities for decoupled sensing and controllable manipulation of our micro-origami can enable broad applications such as end e ectors for testing soft matter and bio materials, micro-robots capable of interacting with their surroundings, haptic sensors for wearable electronic skins, surgical tools, responsive metamaterials, and more.

2 | RESULTS

2.1 | Design and Folding Capability

Figure 1B introduces the design and fabrication of the mixed-transducer micro-origami systems. In this micro-origami design, we combine strained morph (SM) and electro-thermal (ET) transducers into one bi-material morph system called electro-thermal strained morph (ETSM) system (see Fig. 1C). These ETSM transducers have two layers: a gold lm at the bottom and a thin SU-8 layer at the top. During fabrication, heat treatment is used to generate residual stress in the thin SU-8 layer. This residual stress is used to achieve 3D assembly after releasing the micro-origami. In addition, the gold lm is patterned as electric heaters so the ETSM system can fold like an electro-thermal actuator. When applying a voltage across the heater circuit, the current will create Joule heating to heat up the ETSM system. Then, because the SU-8 layer has a larger thermal-expansion coe cient than the gold layer, this ETSM actuator will bend toward the gold side to produce large and active folding motion.

Figure 1D shows design of the thin- lm PZT transducer system. This micro-transducer system contains four layers of materials: a top Pt electrode, a PZT layer, a bottom Pt electrode, and a SiO_2 lm. When a voltage is applied across the top and bottom electrodes, the PZT layer will develop compressive strain. In this case, the SiO_2 lm will serve as a passive layer to generate strain mismatch for folding motion. To ensure robust and secured electric connection, an SU-8 encapsulation layer and a sputtered gold layer are used to build an electrical jumper to connect to the top Pt electrode.

The fabrication process of the mixed-transducer micro-origami is summarized in Fig. 1B and the details can be found in the Materials and Methods and Supplementary Text Section S2. Fabrication starts with a purchased Si wafer with a PZT material stack containing an un-patterned top Pt electrode, PZT layer, bottom Pt electrode, and SiO_2 layer. The four layers are patterned using standard photolithography processes and ion-milling. Next, a gold layer is deposited using electron-beam evaporation and patterned by lift-o . After that, a thin SU-8 layer is patterned using a standard contact lithography process. The gold and the SU-8 layers form the structure of the electro-thermal strained morph (ETSM) transducers. Following the deposition of the thin SU-8 layer, a top gold electrode layer is deposited using Lab Line sputter tool and patterned by wet etch. This sputtered gold layer is used to provide electrical connection

Author Manuscript

This article is protected by copyright. All rights reserved.

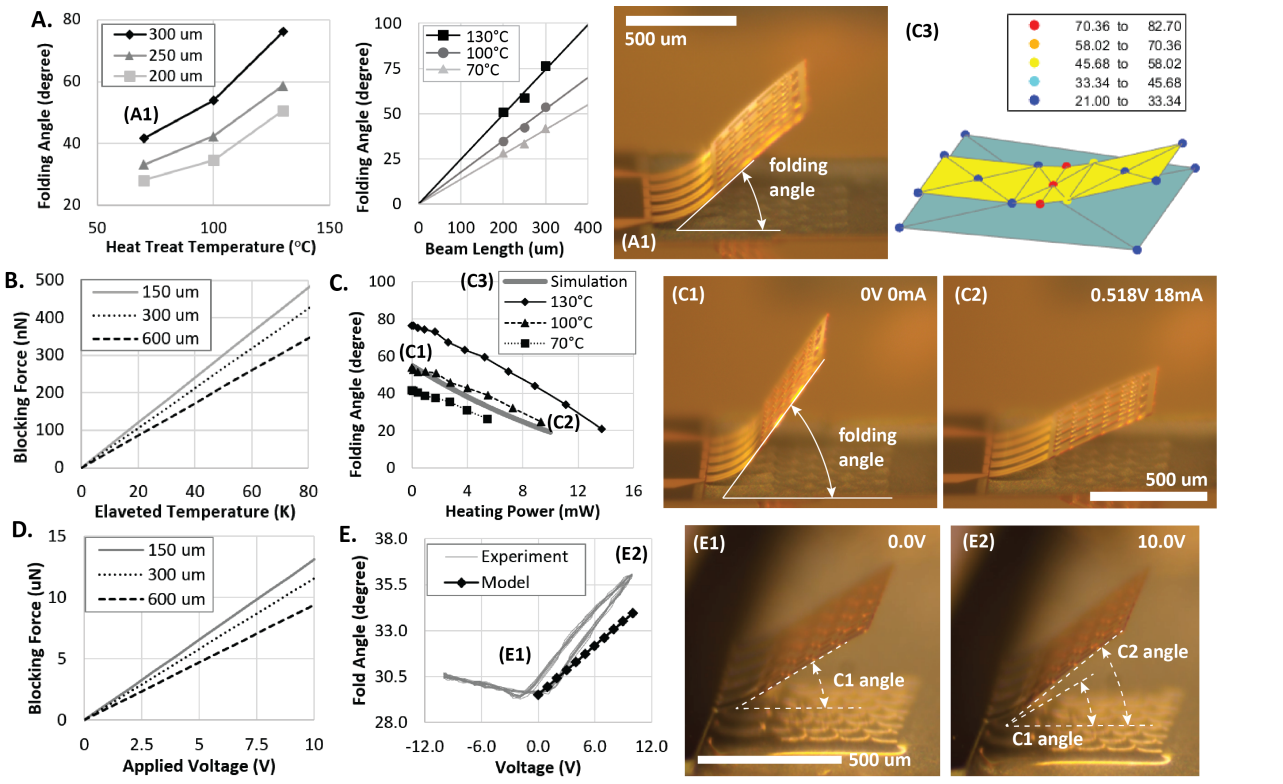


FIGURE 2 Folding capability of the ETSM and PZT systems A. Self-assembly behavior of ETSM system. The plot shows the self-folding angle with respect to the actuator length and the pre-release heat treatment temperature. The heat treatment time is fixed at 10 minutes. **B.** Calculated force output of the ETSM system with respect to the actuator length and the applied temperature. **C.** Active folding angle of ETSM system with respect to the applied heating power. Three micro-origami with the same actuator length (300 µm) but with different heat treatment temperatures are shown. C3 shows a simulation of the multi-physical active folding for the ETSM system. **D.** Calculated force output of the PZT system with respect to the actuator length and the applied voltage. **E.** Active folding angle of the PZT Actuator with 150 µm long beams. The plot shows the measured folding hysteresis of the PZT system under a sine wave input signal and the folding motion from an analytical model with linear material response assumptions. All the flat panels in this figure are 500 µm by 500 µm.

to the top electrode of the thin-film PZT system. Finally, a 5 µm thick SPR220 film is deposited and patterned to serve as the panel(s) of micro-origami structures, and the entire micro-origami is released using XeF_2. After releasing the samples, these micro-origami devices are packaged using the method summarized in Supplementary Text Section S3. By adjusting the origami design and placing the ETSM and PZT transducers at different locations, a variety of micro-origami systems can be produced with customizable geometry, actuation, and sensing capability.

Figure 2A summarizes the self-folding capability of the ETSM system. Before releasing the micro-origami system, a 10 minute pre-release heat treatment is applied to drive away moisture and further cure the SU-8 polymer. This heat treatment builds up residual stress within the bi-material morph and causes the subsequent folding motion for 3D self-assembly. To control the folding angle, one can adjust the length of ETSM system and/or the heat treatment temperature. Longer beams will produce larger folding angles without changing the curvature and the residual stress within the morph. On the contrary, raising the heat treatment temperature can generate more residual stress to produce larger folding angles without increasing the length of the folding creases. Figure 2A also shows that the residual stress and curvature are primarily affected by the heat treatment temperature and not by the beam length.

Author Manuscript

This article is protected by copyright. All rights reserved.

When fixing the heating temperature, the relationship between the folding angle and the beam length is linear. Using the data shown in Fig. 2A, one can select the right combination of heat treatment temperature and crease length to achieve the desired self-assembly.

The ETSM system can also actively "unfold" back to the flat state using electro-thermal actuation after self-assembling into the 3D configuration (see Fig. 1C). Figure 2B shows the relationship between the output force (blocking force), the applied heating temperature, and the actuator length. This ETSM system can produce forces between 10 nN to 500 nN range depending on the applied heating. An analytical model is developed in the Supplementary Text Section S4 to solve for the output forces based on the geometry and the applied heating. The associated modeling procedure was developed in [44] and is verified against experiments. Figure 2C further shows the relationship between the folding angle and the input heating power. As the applied power increases, the panel will actively fold back to flat, and the active folding angle is linearly related to the applied heating power. In addition, Fig. 2C shows that curves with different heat treatment temperatures are parallel to each other, indicating that the active folding motion is not affected by the residual stress and the heat treatment. A multi-physical simulation is used to capture the behavior of the ETSM system and good agreement is obtained for the selected 100°C heat treatment case. This simulation is based on a bar and hinge model for electro-thermal micro-origami [44]. Supplementary Text Section S4 provides further details regarding the implementation of this simulation. The thermal expansion coefficient of both gold and SU-8 materials can be obtained from prior research [45] The results shown in Fig. 2C is based on a single crease origami with 300 µm long actuators and a folding panel with a 500 µm by 500 µm footprint. These dimensions are picked because they can produce a balanced behavior between large folding motion and large output force based on the results shown in [24]. Here, the new ETSM system has a reversed sequence of the gold and SU-8 layers, having gold at the bottom (versus at top as in [24]), so that we can utilize the SU-8 residual stress to achieve self-assembly.

Finally, Fig. 2D-E show the folding capability of the thin-film PZT system. Figure 2D shows the output force (blocking force) of the thin-film PZT actuator with respect to the applied voltage using an analytical model developed in Supplementary Text Section S4. This modeling procedure is based on an experimentally verified model developed in [30]. Compared to the ETSM system, the PZT actuator can achieve a much larger output force in the range of µN, but suffers from a smaller folding range. To study the folding capability of the PZT actuator, we applied a sine wave signal with 10-second period and -10.0V to +10.0V peak-to-peak voltage onto the single-crease origami and measured the folding angle using microscope videos. Fig. 2E shows that the PZT actuator system has a strong asymmetric hysteretic behavior. A relatively larger folding motion is obtained when applying a positive voltage, but a much smaller folding motion is generated (in the same direction) when applying a negative voltage. This asymmetric hysteresis is typical for thin-film piezoelectric actuators [30]. Figure 2E also shows a comparison between the experiment and an analytical model developed in Supplementary Text Section S4. As shown, a good agreement is obtained between the experiment and the model. Because the actuation is based on inverse piezoelectric effect, the energy conversion efficiency of thin film PZT is high. In addition, these thin-film PZT actuators can also achieve high-frequency vibration (more than 500Hz) that is not possible with non-piezoelectric systems. We will demonstrate this high-frequency capability in the next section. The experiments shown in Fig. 2 is based on a single crease device with a 500 µm by 500 µm panel and a 150 µm long PZT actuator. The dimensions of the actuators are selected to produce power efficient motion with good force output based on suggestions from prior research [30].

2.2 | Efficient and Durable Vibration

The proposed micro-origami system can produce high-speed vibration with high power efficiency and good durability. First, we focus on a two-crease micro-origami with a PZT actuator at the base and a ETSM system at the outer crease

This article is protected by copyright. All rights reserved.

Author Manuscript

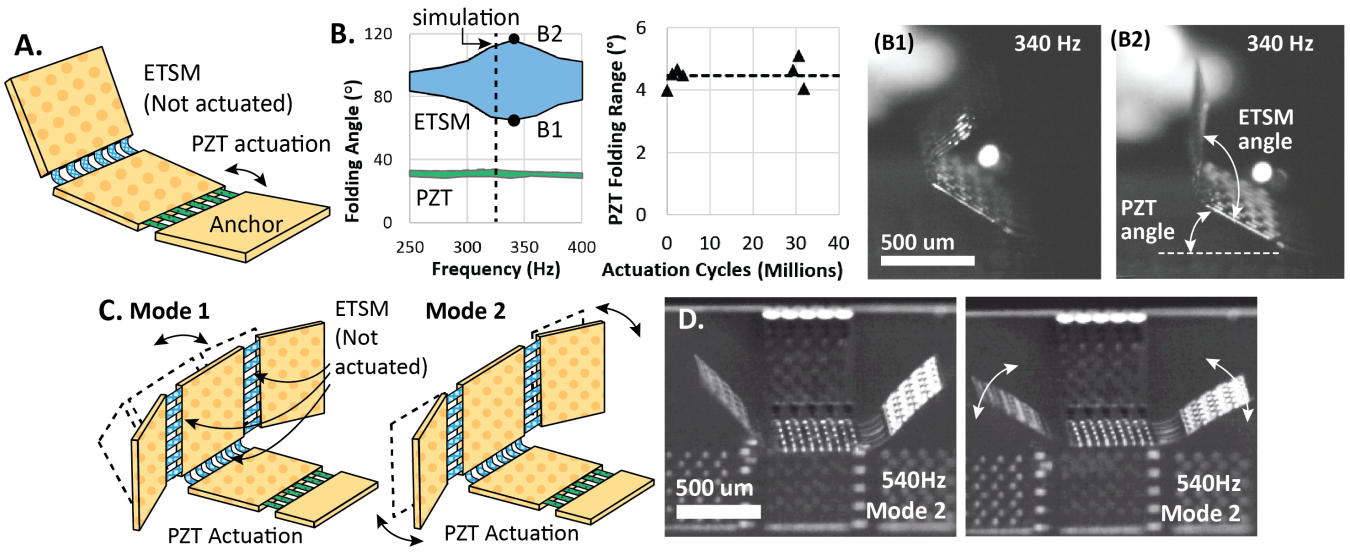


FIGURE 3 **E cient dynamic vibrations. A.** A mixed-transducer micro-origami system with two creases. **B.** Left plot shows the sweeping test results for the folding angle of both PZT and ETSM creases. The shaded region represents the motion range of the two creases under di erent excitation frequency. A fundamental frequency of 340 Hz is identi ed from the experiments. A simulated fundamental frequency of 323 Hz is obtained and marked using dotted lines. Right plot shows the duration test results where the two-crease micro-origami is vibrated for 30 million cycles with no obvious degradation. **C.** Micro-origami structures with multiple creases can achieve complex dynamic folding motions when a single PZT component is actuated at di erent frequencies. **D.** Microscope image of di erent mode shapes for the structure in C. See Supplementary Videos S1 for animation of the devices shown in this gure.

(Fig. 3A). In this design, the ETSM system is used to dynamically amplify the high frequency vibration of the PZT actuator. Figure 3B shows a frequency sweep experiment to study the dynamic ampli cation. A sine wave input with peak-to-peak voltage between 0V to 10V is applied to the PZT actuator, while folding angles of both creases are tracked using a high speed camera. The motion range of the ETSM crease reaches its maximum when the input PZT motion aligns with the fundamental frequency of the system (at 340 Hz). At resonance, the ETSM crease is folding at 340Hz and has a folding angle range of about 50 degrees. This corresponds to a folding speed of 17,000 degree per second, which is almost two-times faster than using the electro-thermal actuation alone [24]. The measured damping ratio of the two-crease micro origami is 0.149. Please see Supplementary Video S1 for animation of this dynamic ampli cation behavior. An analytical model is built in the Supplementary Text Section S5 to capture the fundamental frequency of this two-crease micro-origami. This analytical model predicts a fundamental frequency of 323 Hz, which is close to the measured value from the frequency sweep experiment.

Moreover, because PZT system has high e ciency in converting electrical power to material strain, our mixed-transducer micro-origami consumes much less power when compared to micro-systems built with only ETSM actuators. Experiments in Supplementary Text Section S6 indicates that typical power consumption of thin- lm PZT systems, operating at around 8V and 200Hz, is between 10 to 40 µW. On the contrary, ETSM actuators with similar sizes require about 10 to 30 mW of power to operate [24], which is around 1,000 times more than using the thin- lm PZT. These measurements highlight the advantage of using micro-origami systems with mixed transducers, where we can combine the large folding capability of the ETSM system and the low power consumption of PZT transducers. In addition, it is possible to program the vibration by sending decoupled input signals into the PZT and ETSM actuators as demonstrated in the Supplementary Text Section S6.

Author Manuscript

This article is protected by copyright. All rights reserved.

Furthermore, the mixed-transducer micro-origami system is highly durable, because both the ETSM and the PZT actuators can fold a large number of cycles with no obvious degradation. The durability of ETSM system is demonstrated in [24], where a single crease electro-thermal actuator is repeatedly folded for over 100,000 cycles with no obvious degradation in motion. Here, we tested the durability of the two-crease origami system with both an ETSM crease and a PZT crease. The thin-film PZT crease is kept vibrating at resonance frequency (340 Hz) for 26 hours, while its motion range is measured every hour during the beginning and the end of the experiments. The PZT actuators are actuated using 10.0V peak to peak voltage and a 5.0V offset. During the measurement, the vibration is temporarily slowed down to 1 Hz (for less than one minute) to obtain the static folding angle of PZT crease, and the results are plotted in Figure 3B. Our results indicate that the PZT crease displays no obvious degradation in its motion range after folding for more than 30 million cycles. Readers may refer to the Supplementary Video S1 to see how the folding capability changes as we fold this mixed-transducer micro-origami system for more than 30 million cycles.

Finally, we show that by integrating more panels into the micro-origami systems, it is possible to generate more complex vibration modes and configurations. The device shown in Fig. 3C is a box-shape origami with three ETSM creases and one PZT crease. This pattern reaches its first vibration mode at 190 Hz. With this model, the origami vibrates its base ETSM crease with little folding in the two vertical ETSM creases. This deisgn has a second vibration mode at 540 Hz, where the two side panels flap with little motion in the base ETSM crease. This motion is similar to the motion of flapping wings in a small-scale inset. Supplementary Video S1 shows the motions of these different modes. Adding more panels can trigger more complicated mode shapes and dynamic motions. We believe the simulation and modeling method demonstrated in Supplementary Text Section S4 and S5 can be used to explore these complex dynamic motions in future research.

Micro-origami systems like devices shown in Fig. 3A and 3C can be used as micro-robotic legs for motions [12] or be used as micro cilia for fluidic flow manipulation [29]. The proposed mixed-transducer micro-origami can achieve more power efficient vibration when compared to purely ETSM micro-systems [24], can achieve more versatile motion directions when compared with purely PZT micro systems [12]. Moreover, the proposed micro-device has a much longer life span compared to related electro-chemical micro-actuators reported in [29, 27] because both the ETSM and the PZT system have little degradation.

2.3 | Controllable and Versatile Motions

Using mixed-transducer can also enable micro-origami systems to achieve controllable and versatile motions that cannot be achieved with a single transduction mechanism. For example, PZT-only micro-robot joints have limited motion versatility. Figure 4A shows two traditional PZT based micro-robot joint designs [43, 30, 46]. Simple PZT actuators can achieve upwards and downwards bending motions as shown in Fig. 4A left. To Achieve in-plane rotational motion with PZT actuators, we need to design special compliant mechanisms as shown in Fig. 4A right [12]. However, even with the special mechanism, the rotational motion range is still limited to a few degrees. Moreover, it is difficult to design micro-robotic joints with PZT actuators to produce folding motion in arbitrary directions.

On the contrary, while micro-robot joints built with ETSM systems offer large folding angles and complex motions, they suffer from thermal coupling which can substantially limit their controllability. Figure 4B shows one robotic leg built with two ETSM creases. When actuating the multi-joint ETSM micro-robot leg, it is difficult to separately control a single ETSM crease due to the thermal coupling between adjacent creases. For example, applying current to the outer ETSM fold f_0 using heater R_0 will unavoidably generate heat in the connection wire R_{01}. This is because physical connection wires within MEMS devices have finite nonzero resistance. Because the connection wire R_{01} is adjacent to the other ETSM fold f_1, the heat generated by R_{01} will inevitably create folding motion in the base fold f_1. Figure 4C

Author Manuscript

This article is protected by copyright. All rights reserved.

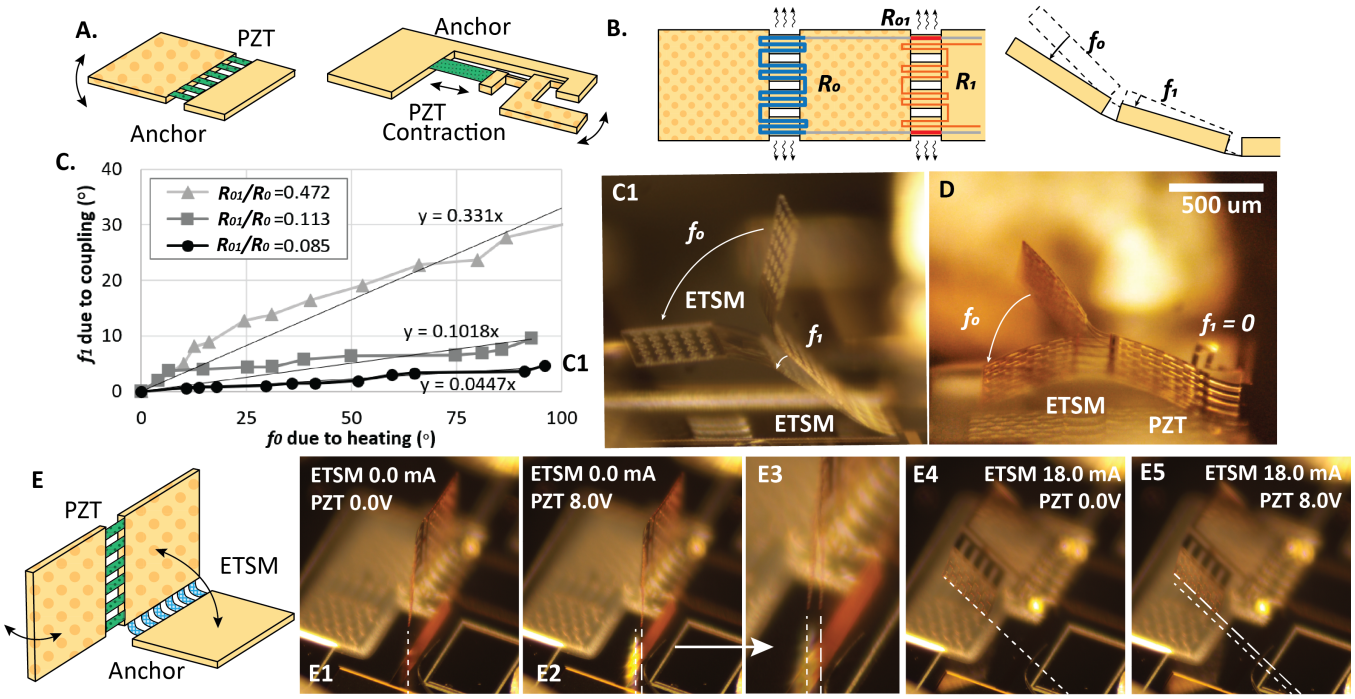


FIGURE 4 **Decoupled transducer for controllable and versatile robotic motions. A.** Traditional thin-film PZT robotic joints have trouble generating versatile motions in multiple planes. Simple joint design can only achieve up and down motion, while in-plane rotational motion requires special compliant mechanisms. **B.** Traditional electro-thermal robotic joints suffer from coupled folding behaviors. Applying heat to fold f_0 also generate heat and a reduced folding motion in fold f_1. R_0 is the resistance of the heating circuit (blue) for fold f_0 while R_1 is the resistance of heating circuit (orange) for fold f_1. R_{01} is the resistance of the connection wire (red) to power fold f_0. **C.** Stronger coupling effects are obtained when the resistance ratio between the connection wire R_{01} and the heater R_0 is larger. C1 shows the deformation when we apply a current in R_0 to fold f_0. Although there is no current in R_1 heater, folding is developed in fold f_1 due to the heat from connection wire R_{01}. **D.** Using mixed-transducer micro-origami can avoid thermal coupling for better motion control. Folding the outer ETSM crease f_0 will not produce motion in the base PZT crease f_1. **E.** Controllable robotic joint with both ETSM and PZT transducers. Dotted lines are used to indicate the motion of the PZT crease. E3 overlays E1 and E2 to show the PZT crease motion. All devices are demonstrated in Supplementary Video S2.

shows this coupling behavior by plotting the folding angle f_1 due to coupling with respect to the active folding angle f_0 due to applied heating for different micro-origami designs. As shown, applying current to fold f_0 will trigger a reduced folding motion in f_1 even when the fold f_1 is not actively actuated (No current in heater R_1). This effect is also demonstrated in Fig. 4C1, where folding the outer ETSM crease f_0 also produces motion in base ETSM crease f_1. Although this coupling effect can be partially mitigated by reducing the resistance of connection wire R_{01}, it is difficult to completely eliminate the effect. More details about this coupling effect can be found in Supplementary Text Section S7. The thermal coupling between folding creases makes it difficult to produce controllable micro-origami systems with multi-degree-of-freedom actuation.

Here, we show that the coupling problem can be resolved by using both ETSM and PZT transducers. Because PZT and ETSM rely on different mechanisms to generate folding motion, there is no coupling between the two. Thus, if we build the base crease using PZT, folding the outer ETSM crease f_0 will produce no motion in the base PZT crease f_1. This is demonstrated in Fig. 4D, where the base panel has no motion when we fold the top panel downward using the ETSM fold f_0. It is beneficial to fully decouple the folding motion of different actuating creases because it makes

Author Manuscript

This article is protected by copyright. All rights reserved.

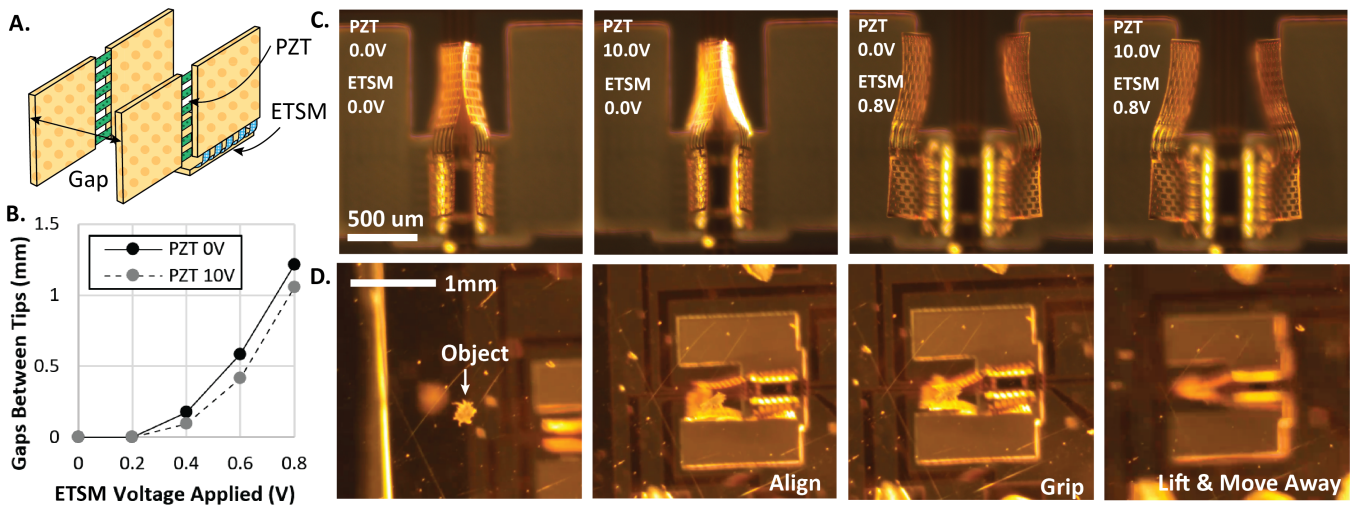


FIGURE 5 **Micro-origami gripper with tunable gripping range. A.** 3D illustration of the micro-origami gripper with two ETSM creases and two thin-film PZT creases. All four creases can be controlled separately (see Supplementary Video S3). **B.** Tunable gripping range with large gap variation enabled by ETSM creases and controllable and decoupled motion enabled by PZT creases. **C.** Micro-scope pictures of the micro-origami gripper with controllable and versatile motion and tunable gripping range. See Supplementary Video S3 for other motions achievable with the gripper. **D.** Mixed-transducer gripper in action: Moving a piece of paper scrap. See Supplementary Video S4 for this experiment.

motion planning easier. Supplementary Video S2 shows a comparison between the coupled ETSM only micro-origami and the decoupled mixed-transducer micro-origami.

In addition, we can also place the PZT at the outer creases and place the ETSM at the base crease. Figure 4E shows this design, where the second PZT crease is also rotated 90 degrees from the base crease. With this micro-robotic joint, the folding motion of both creases are still decoupled. Moreover, this design can provide more versatile motions when compared to a PZT only micro-system. Once this design is released and folded to an assembled state, we can use electro-thermal actuation to alter the position of the thin-film PZT crease to produce PZT folding motion at arbitrary nominal angles. Figure 4E and Supplementary Video S2 shows the different configurations achievable by changing the input current into the ETSM crease. Applying current to the ETSM will fold the joint back to the flat configuration. Figure 4E1 and 4E2 show the PZT motion when ETSM has 0 mA input current, while Fig. 4E4 and 4E5 show the PZT motion when ETSM has 18 mA input current. At these different applied currents, the thin-film PZT joint can be folded to different orientations and be actuated by applying an independent voltage (8.0V DC for the test in the figure). The motion of the PZT crease is illustrated using different doted lines in Fig.4E. The capability of producing PZT vibration at arbitrary angles is not possible with PZT only micro-robots, highlighting the benefit of using mixed-transducers. Furthermore, both PZT crease and ETSM crease can be actuated separately with controllable motion and no coupling effects, which is a benefit that cannot be achieved with ETSM only micro-robots.

Next, we introduce a functional micro-gripper device to highlight the versatility and the controllability of the proposed mixed-transducer micro-origami system. Figure 5A shows an illustration of this 3D micro-gripper. This gripper design contains four actuation creases (two ETSM and two PZT), where all four creases can be controlled individually to achieve complex motions (see Supplementary Video S3). Upon release, the two ETSM creases will fold the gripper to its 3D state. The two PZT creases can achieve decoupled and controllable gripping motion while the two ETSM creases can produce large folding angles to adjust the gripping range. Because there is no coupling

Author Manuscript

This article is protected by copyright. All rights reserved.

behavior between the ETSM and PZT creases, it is easy to control the motion of this gripper. If the two PZT creases are made with ETSM systems, applying current to close the gripping arm will also generate motion in the base creases to change the overall con□guration of the gripper. The coupling behavior is more severe for this gripper design when compared to the devices in Fig. 4B. This is because the outer crease for the gripping arm (equivalent to the f_0 crease in Fig. 4B) is closer to the base crease (equivalent to the f_1 crease in Fig. 4B) - the heat from outer crease can directly heat up the base crease. This thermal coupling behavior is not ideal for achieving robust motion control.

Figure 5B shows the measured gripping range of the mixed-transducer gripper with respect to the applied voltage at the ETSM creases. Figure 5C shows microscope images of the gripper functioning at di□erent con□gurations. When a small current is applied to the ETSM creases, the tips of gripping arms are closely spaced. However, when applying a large current to the ETSM creases, the gripper provides a larger distance between the gripping arms. Moreover, the initial con□guration (0.0V input) can be adjusted by changing the heat treatment temperature before release. Figures 5B and 5C show an example with high heat treatment temperature. In this case, the gripper tips are touching each other when no input current is applied. Having gripper arms touching each other when there is no input applied to the ETSM system is useful because it enables larger gripping forces so that the system can hold an object without an input power. In addition to achieving a tunable folding range, we can separately control the motion of all four creases within this gripper. Supplementary Video S3 highlights this high versatility and controllability of this gripper design. Each gripper arm can be actuated separately to produce out-of-phase motions or in-phase motions depending on the needs. The operation frequency of the gripping arm can also be controlled separately, which o□ers greater □exibility and controllability when compared to grippers using only the ETSM systems.

Finally, Fig. 5D and Supplementary Video S4 shows how we can use this mixed-transducer micro-origami gripper to manipulate small objects. The target object is a paper scrap as shown in Fig. 5D and the manipulation stand of this micro-gripper system is shown in Supplementary Text Section S3. The origami gripper is mounted to a XYZ micro-manipulator. In this experiment, we can move the gripper around using the micro-manipulator, can adjust the input voltage for gripping the object, and can use the gripper to lift and move the object. The output forces of the two actuation creases are shown in Fig. 2. With both ETSM and PZT actuators, the output forces are in the range between 100 nN to 10 uN. This test highlights the superior actuation capability of the proposed micro-origami systems in atmospheric environments, which is useful for building micro-manipulators, assembling small-scale engineered systems, manipulating micro-scale bio samples, and for other applications.

2.4 | Decoupled Sensing

In addition to achieving e□ cient vibration and controllable motion, mixed-transducer micro-origami systems can also accomplish decoupled sensing. Because the ETSM system is decoupled from the thin-□lm PZT transducer, it is possible to use the ETSM transducer as a strain gauge to measure the folding angle while simultaneously actuating the micro-origami using the thin-□lm PZT transducer. These ETSM strain gauges use piezoresistive sensing mechanisms. When a ETSM crease is bent, it will stretch or shorten the gold circuit and change the total resistivity. The changing resistivity can be measured using a Wheatstone bridge and an ampli□cation circuit, so that we can use the sensor reading to infer the folding angle (see details in Supplementary Text Section S8).

In this subsection, the decoupled sensing capability is demonstrated using the same two-crease micro-origami introduced in Fig. 3. We show that the two-crease origami can sense (1) its own folding motion and (2) the interaction with small-scale samples. To demonstrate the capability of sensing the folding motion, we vibrate the micro-origami using the PZT crease to produce ampli□ed motion in the ETSM crease. This vibration will change the resistivity of the ETSM crease, which is detected using an amplifying circuit, as listed in Supplementary Text Section S8. The sensor

Author Manuscript

This article is protected by copyright. All rights reserved.

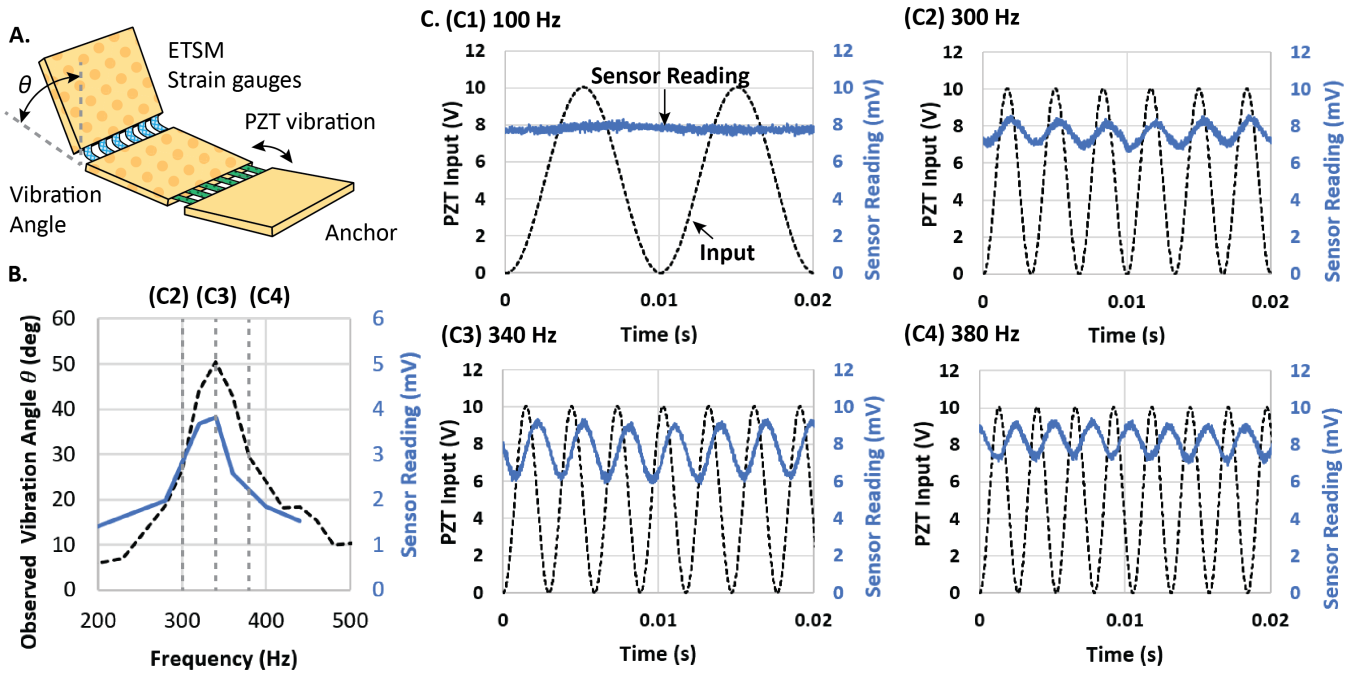


FIGURE 6 **Decoupled transducer for simultaneous actuation and sensing. A.** Using ETSM crease as strain gauges to sense the folding motion. **B.** Comparing the measured angle θ from high speed video with sensor reading for a sweeping test. Larger sensor reading (in mV) indicates larger strain value and larger folding angle. Blue solid line is for sensor reading and black dotted line is for observed folding angle. **C.** Comparison between the PZT input signal and signal reading from ETSM sensor. At 100 Hz, there is no dynamic ampli□cation so the ETSM sensor picks up noise. At 340 Hz, resonance occurs and the ETSM sensor picks up the strongest signal. Blue solid line is for sensor reading and black dotted line is for PZT input signal.

reading gives us a reference to infer the vibration motion in the mixed-transducer micro-origami. Figure 6B shows a comparison between the vibration angle measured from the high-speed camera videos and the sensing signals from a frequency sweep experiment. We can see from the comparison that the shape of the sensor signal matches the shape of the measured folding angle relatively well and predicts the same resonance frequency at 340 Hz. Figure 6C further shows the time history comparison between the input PZT driving signal and the sensor reading. At 100 Hz input, there is limited active vibration and the sensor output is dominated by noise. At 340 Hz input, the device vibrates near its □rst resonance frequency and a strong sensor output is recorded. As we move away from the resonance to 300 Hz and 380 Hz, we can see output attenuation and phase shifts captured accurately by the internal ETSM sensor. The Supplementary Video S5 shows a comparison between the sensor reading and the recorded folding motion from a high-speed camera.

In addition to sensing folding angle, these mixed-transducer micro-origami can also pick up signals when interacting with external environments or small-scale objects (see Fig. 7A). Figure 7B shows that the mixed-transducer micro-origami can pick up di□erent signals when interacting with di□erent samples. In this experiment, we maintain a 2Hz vibration in the thin-□lm PZT actuator and bring the micro-origami in contact with di□erent objects, including a plant □ber (watermelon pulp) and a copper wire. We can see from Fig. 7B that di□erent sensor signals are generated when the micro-origami is touching di□erent objects. When touching the plant □ber, we pick up a strong sine wave signal as the transducer and object compliance are similar and maintain contact; when touching the copper wire, we pick up a wave form that is close to a square wave as impact, hold, then detachment occurs in each cycle; When no

Author Manuscript

This article is protected by copyright. All rights reserved.

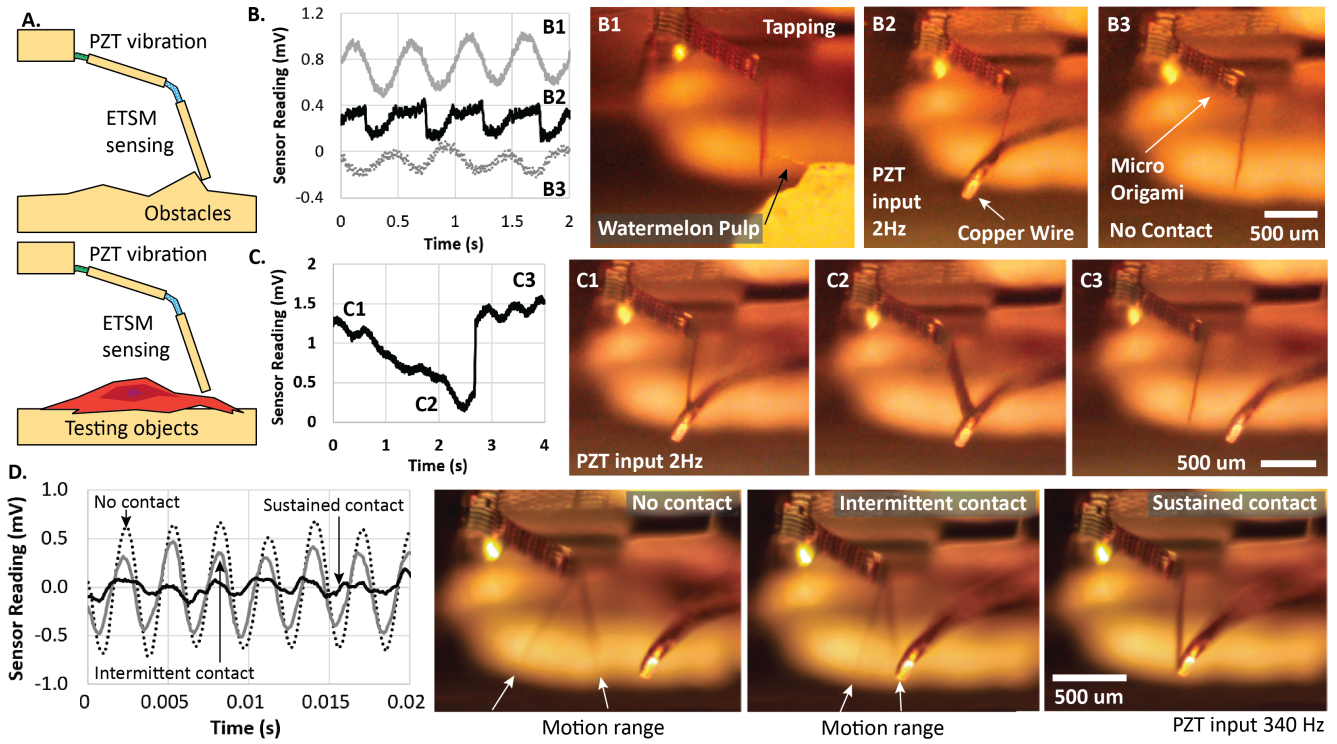


FIGURE 7 **Sensing interactions between the micro-origami and the surrounding environment. A.** Setup for testing the how the mixed-transducer origami can interact with external environments and small-scale samples. **B.** The mixed-transducer micro-origami picks up different wave forms when interacting with (B1) watermelon pulp, (B2) a copper wire, and (B3) nothing. **C.** The system can sense engagement and disengagement of contact with a copper wire. **D.** In rapid dynamic testing, the ETSM sensor can pick up different vibration signals when the copper wire alters the micro-origami vibration through intermittent contact and sustained contact. All experiments are demonstrated in supplementary video S6.

contact is happening, the sensor can pick up a weak sine wave signal.

Figure 7C shows another signal we picked up when the micro-origami disengage from contacting with a copper wire. In this experiment, we maintain a 2 Hz vibration in the PZT crease and slide a copper wire across the micro-origami. As the copper wire moves away from the micro-origami, it first pushes the micro-origami to develop a big deformation and produces a strong signal. Then, the contact disengagement occurs and the two-crease micro-origami snaps back to its original position. Although the snapping occurs rapidly, the sensor can still pick up the sharp transition in motion. This is because the sensing circuit can pick up signals at a sampling rate of 100 kHz or higher, which is much faster than common microscope cameras or even high-speed microscope cameras. In our experiment, we use a sampling rate of 250 kHz.

Finally, we want to highlight the capability to sense the interaction with the external environment in a dynamic context with a high sampling rate. In this experiment, we vibrate the PZT at 340 Hz (resonance frequency) and use a copper wire to push against the vibrating panel. Figure 7D shows the sensing signal and the vibration motion of the two-crease micro-origami. At this high frequency, standard micro-scope videos can only capture a blurred shadow of the moving system, illustrating the limitation of video based sensing methods for small-scale target. However, our decoupled strain gauge sensor system can easily achieve a sampling rate higher than 100 kHz to measure the motion of the micro-origami. Our data show that contact can change both the amplitude and wave form of the sensing signal. When no contact is initiated, the sensor picks up the strongest signal and a standard sinusoidal wave form. When a

Author Manuscript

This article is protected by copyright. All rights reserved.

weak and intermittent contact is initiated, where the copper wire just gently touches the two-crease micro-origami, the sensor picks up a sinusoidal signal with reduced magnitude. When a sustained contact is initiated, the signal magnitude is drastically reduced and there is no longer a clear sinusoidal vibration wave form.

The capability to simultaneously perform sensing and actuation is a substantial advantage for a mixed-transducer micro-origami system when compared to micro-devices reliant on a single transduction mechanism. Because the di erent transducers are decoupled in the electrical domain, there is limited interference between actuation and sensing, so that the device can obtain clean sensing signal while simultaneously achieving actuation. This decoupled sensing capability is bene cial for many applications. For example, when using the micro-origami to build robotic legs, we can use the sensing signal to understand how the legs are interacting with external environments. In addition, we can use these micro-origami to probe the mechanical characteristics of cells and biomedical samples. We can collect sensing data while actively interacting with and stimulating the objects of interest.

3 | DISCUSSION AND CONCLUSION

In summary, this work introduces a mixed-transducer micro-origami system that can achieve controllable motion, e cient vibration, and decoupled sensing. We designed an ETSM transducer and a PZT transducer for the mixed-transducer micro-origami so that it can organically combine the self-assembly capability of SM systems, the large folding and sensing capability of ET systems, and the power e cient and durable vibration capability of PZT systems. A versatile micro-fabrication procedure is developed to build the proposed mixed-transducer micro-origami using photolithography processes. The folding performance of these mixed-transducer micro-origami are investigated using analytical models, simulations, and experiments. We rst show that the proposed micro-origami can achieve power e cient and highly durable vibration (with no obvious degradation after 30 million cycles). Next, we demonstrate that these micro-origami can produce controllable and versatile motion with no coupling e ects between folding creases. Finally, these micro-origami can sense their folding motion and interaction with surrounding environments or small-scale bio samples. Because the ETSM sensor is decoupled from the PZT system, clean sensor readings can be obtained at high sampling rates.

More importantly, this work demonstrates the usefulness of building micro-origami systems and micro-robotic systems with mixed-transducers: using multiple transducers can overcome the inherent limitation of single transducer systems, achieving decoupling in the electrical domain for better motion control and sensing capability. In the future, new micro-fabrication processes can be developed to combine other transducer systems into micro-origami systems to accomplish more complex functionality. We envision that the demonstrated micro-origami (such as the device in Fig. 7) provides powerful end-e ectors to probe the mechanics of bio samples and soft matter. These systems can also be used to build power e cient micro-robotic legs for motion or functional micro-cilia for manipulation. Furthermore, we could potentially use these micro-origami as haptic sensors in soft skins or wearable electronics, because they can collect clean sensing signals at high sampling rate.

Experiments and Methods

| Fabrication of Mixed Transducer Micro-Origami

Figure S1 in the Supplementary Text shows the detailed fabrication process. The process starts with a Si wafer with deposited PZT layers on one surface (purchased from Radiant Technologies Inc). The information of these layers (from top to bottom) are as follows: top Pt electrode 0.15 µm, 52/48 PZT 1 µm, bottom Pt electrode 0.15 µm, TiO_2 0.04 µm,

Author Manuscript

This article is protected by copyright. All rights reserved.

SiO2 0.5 µm. The additional TiO_2 layer is added to help with adhesion based on the recommendation from Radiant Technologies Inc. The top Pt, PZT, bottom Pt, and TiO_2 layers are patterned using Nanoquest II Ion-mill (Intlvac Thin Film) and the SiO_2 layer is patterned using an STS APS DGRIE (STS Glass Etcher) tool (SPTS Technologies) at Lurie Nanofabrication Facility (LNF) at the University of Michigan. The mask material for the Pt layers is Photoresist S1813 (1.0 µm) and the mask material for the PZT layer and the Silicon Dioxide layer is the SPR 220 (3.0) photoresist (3.0 µm).

After patterning the PZT material stack, the next step is to pattern a bottom gold layer for creating the ETSM actuator system. This gold layer is patterned using a lift-o process with the LOR 10B (Kayaku Advanced Materials) and S1813 photoresist (Shipley). After patterning the lift-o resist, 0.2 µm of gold with an adhesion layer of 0.02 µm Cr is deposited using the Evovac Evaporator (Angstrom Engineering) at LNF. The lifto is then accomplished using the Remover PG (Kayaku Advanced Materials).

Next, a thin layer (0.8 µm) of SU-8 2000.5 (Kayaku Advanced Materials) is deposited on top of the wafer. The spin speed, baking time, and exposure dosage is calculated using the data sheet provided by the manufacturer. To obtain a high quality SU-8 lm with good adhesion, it is recommended to add additional exposure dosage to help promote the bonding strength. After patterning the SU-8 thin lm, a 10 min hard bake at 150 °C is recommended to fully crosslink the SU-8 layer for improving lm quality. After hard baking the SU-8 lm, a top gold lm (0.2 µm) is deposited using the Lab Line sputter tool (Kurt J. Lesker Company) and patterned using Gold Etch GE-8111 (Transene Company). The etch rate is determined using the data sheet provided by the etchant manufacturer. When depositing this top gold layer, it is not necessary to add an adhesion layer because gold tends to bond well with SU-8 [47]. Next, we pattern a 5 µm thick SPR 220 (3.0) photoresist to create the panels that connects di erent actuator systems. Finally, the micro-origami is released using XeF_2. More information about this micro fabrication can be found in the Supplementary Text Section S2.

| Modeling of Actuation

This work uses both analytical model and simulation to capture the folding behaviors in ETSM system and PZT system. For the ETSM system, the active folding is generated using electro-thermal actuation. We can use a bar and hinge model to nd the elevated temperature based on the input power [44]. After nding the elevated temperature, a bi-material beam model developed by Timoshenko can be used to compute the active folding motion [48]. Finally, the blocking forces can be computed using the composite bending rigidity of the actuator. For the PZT system, the material strain is related with the applied voltage through a material constant, a piezoelectric strain coe cient d_{31} [49]. This strain can be converted to an active moment using the material properties and geometry of actuator layers. With the active moment, we can further compute the blocking force and the motion range of the PZT system. Details about these modeling processes can be found in the Supplementary Text Section S4. A supplementary code package is provided to implment the simulation shown on Fig. 2C3.

| Sensor Testing

Figure S13 in the Supplementary Text shows the circuit design for obtaining the sensor reading when using ETSM transducers as piezoresistive sensors (Fig. 6 and Fig. 7). This circuit consists of a Wheatstone bridge and an ampli- cation circuit. The sensor readings are directly measured using NI DAQ and LabView. A MATLAB code is used to process the sensor results, and a moving average with 15 time steps is used to smooth the data. The sampling rate is 250 kHz, which is much higher than the major modal frequencies of the vibration systems shown in Fig. 3 and Fig. 6.

Author Manuscript

This article is protected by copyright. All rights reserved.

Further details about the sensor testing can be found in Supplementary Text Section S8.

| High Speed Video Recording

A Photron Fastcam MC2.1 camera system is used to record the high frequency vibration of the micro-origami. The recording frequency is set such that each frame can capture a still image that is not blurry. This usually required us to use a frame rate that is 10 to 20 time the actuation frequency of the input signal. The highest frame rate used in this research is 4000 FPS. When recording the videos, strong light sources are used to illuminate the samples for good image quality. The folding angle is measured using the high-speed video and a software tool kit called Tracker v6.0.8. The input signal is applied using an AC source meter (Tektronix AFG 1022) and the voltage time history is directly measured from the source meter.

Acknowledgments

The authors thank all sta members from the Lurie Nanofabrication Facility for their helpful advice on micro-fabrication processes. We also appreciate the helpful discussion and suggestions from Dr. M. Birla at the the early stages of this work. We would like to thank the reviewer for their comments and suggestions.

references

[1] Q. Jin, Y. Yang, J. A. Jackson, C. Yoon, D. H. Gracias, *Nano Letter* **2020**, *20* 5383.

[2] E. W. H. Jager, O. Inganas, I. Lundstrom, *Science* **2000**, *288* 2335.

[3] J. K. Luo, J. H. He, Y. Q. Fu, A. J. Flewitt, S. M. Spearing, N. A. Fleck, W. Milne, *Journal of Micromechanics and Microengineering* **2005**, *15* 1406.

[4] J. Luo, R. Huang, J. He, Y. Fu, A. Flewitt, S. Spearing, N. Fleck, W. Milne, *Sensors and Actuators A* **2006**, *132* 346.

[5] F. Beyeler, A. Neild, S. Oberti, D. J. Bell, Y. Sun, J. Dual, B. J. Nelson, *Journal of Microelectromechanical Systems* **2007**, *16* 7.

[6] T. G. Leong, C. L. Randall, B. R. Benson, N. Bassik, G. M. Stern, D. H. Gracias, *PNAS* **2009**, *106* 703.

[7] K. Kuribayashi, K. Tsuchiya, Z. You, D. Tomus, M. Umemoto, T. Ito, M. Sasaki, *Materials Science and Engineering: A* **2006**, *419* 131.

[8] J. C. Breger, C. Yoon, R. Xiao, H. R. Kwag, M. O. Wang, J. P. Fisher, T. D. Nguyen, D. H. Gracias, *ACS Applied Materials and Interfaces* **2015**, *7*, 5 3398.

[9] J. L. Silverberg, J.-H. Na, A. A. Evans, B. Liu, T. C. Hull, C. D. Santangelo, R. J. Lang, R. C. Hayward, I. Cohen, *Nature Materials* **2015**, *14* 389.

[10] Z. Lin, L. S. Novelino, H. Wei, N. A. Alderete, G. H. Paulino, H. D. Espinosa, S. Krishnaswamy, *Small* **2020**, *16* 2002229.

[11] Y. Liu, Z. Gao, K. Liu, T. Wu, In *2021 21st International Conference on Solid-State Sensors, Actuators and Microsystems (Transducers)*. **2021** .

[12] J. Choi, M. Shin, R. Q. Rudy, C. Kao, J. S. Pulskamp, R. G. Polcawich, K. R. Oldham, *Int. J. Intell. Robot. Appl.* **2017**, *1* 180.

[13] T. G. Ivanov, J. S. Pulskamp, R. G. Polcawich, R. M. Proie, In *2012 IEEE/MTT-S International Microwave Symposium Digest, 17-22 June 2012, Montreal, QC, Canada*. **2012** .

Author Manuscript

This article is protected by copyright. All rights reserved.

[14] J. S. Pulskamp, R. G. Polcawich, R. Q. Rudy, S. S. Bedair, R. M. Proie, T. Ivanov, G. L. Smith, *MRS Bulletin* **2012**, *37* 1062.

[15] E. Iwase, I. Shimoyama, *Journal of Microelectromechanical Systems* **2005**, *14* 1265.

[16] N. S. Shaar, G. Barbastathis, C. Livermore, *Journal of Microelectromechanical Systems* **2015**, *24* 1043.

[17] M. Z. Miskin, A. J. Cortese, K. Dorsey, E. P. Esposito, M. F. Reynolds, Q. Liu, M. Cao, D. A. Muller, P. L. McEuen, I. Cohen, *Nature* **2020**, *584* 557.

[18] M. Ataka, A. Omodaka, N. Takeshima, H. Fujita, *Journal of Microelectromechanical Systems* **1993**, *2*, 4 146.

[19] Y. Zhang, B. K. Chen, X. Liu, Y. Sun, *IEEE Transactions on Robotics* **2010**, *26* 200.

[20] Z. Li, M. Li, Q. Fan, X. Qi, L. Qu, M. Tian, *ACS Applied Materials and Interfaces* **2021**, *13* 14778.

[21] M. Li, Z. Li, L. Qu, F. Chen, M. Tian, *Adv. Fiber Mater.* **2022**, *4* 1005.

[22] M. Li, Z. Li, X. Ye, W. He, L. Qu, M. Tian, *Advanced Functional Materials* **2022**, *33* 2210111.

[23] H. Zhao, X. Qi, Y. Ma, X. Sun, X. Liu, X. Zhang, M. Tian, L. Qu, *ACS Nano Letters* **2021**, *21* 8126.

[24] Y. Zhu, B. Mayur, K. R. Oldham, E. T. Filipov, *Advanced Functional Materials* **2020**, *30*, 2003741.

[25] J.-H. Na, A. A. Evans, J. Bae, M. C. Chiappelli, C. D. Santangelo, R. J. Lang, T. C. Hull, R. C. Hayward, *Advanced Materials* **2015**, *27* 79.

[26] J.-H. Kang, H. Kim, C. D. Santangelo, R. C. Hayward, *Advanced Materials* **2019**, *31*, 0193006.

[27] Q. Liu, W. Wang, M. F. Reynolds, M. C. Cao, M. Z. Miskin, T. A. Arias, D. A. Muller, P. L. McEuen, I. Cohen, *Science Robotics* **2021**, *6*, eabe6663.

[28] J. Rogers, Y. Huang, O. G. Schmidt, D. H. Gracias, *MRS Bulletin* **2016**, *41* 123.

[29] W. Wang, Q. Liu, I. Tanasijevic, M. F. Reynolds, A. J. Cortese, M. Z. Miskin, M. C. Cao, D. A. Muller, A. C. Molnar, E. Lauga, P. L. McEuen, I. Cohen, *Nature* **2022**, *605* 681–686.

[30] Z. Qiu, J. S. Pulskamp, X. Lin, C.-H. Rhee, R. G. P. Thomas Wang, K. R. Oldham, *J. Micromech. Microeng.* **2010**, *20*, 075016.

[31] W. Pang, S. Xu, L. Liu, R. Bo, Y. Zhang, *Advanced Intelligent Systems* **2023**, 2300060.

[32] S. Leanza, S. Wu, X. Sun, H. J. Qi, R. R. Zhao, *Advanced Materials* **2023**, 2302066.

[33] K. Kubota, T. Fleischmann, S. Saravanan, P. O. Vaccaro, T. Aida, *Jpn. J. Appl. Phys.* **2003**, *42* 4079.

[34] N. Bassik, G. M. Stern, D. H. Gracias, *Applied Physics Letters* **2009**, *95*, 091901.

[35] E. Moiseeva, Y. M. Senousy, S. McNamara, C. K. Harnett, *J. Micromech. Microeng.* **2007**, *17* N63.

[36] W. J. Arora, A. J. Nichol, H. I. Smith, G. Barbastathis, *Applied Physics Letters* **2006**, *88*, 053108.

[37] A. Arevalo, D. Conchouso, D. Castro, M. Diaz, I. G. Foulds, *Micro & Nano Letters* **2015**, *10* 545.

[38] J. W. Suh, R. B. Darling, K.-F. Bohringer, B. R. Donald, H. Baltes, G. T. A. Kovas, *Journal of Microelectromechanical Systems* **1999**, *8*, 4 483.

[39] N. J. Conway, Z. J. Traina, S.-G. Kim, *Journal of Micromechanics and Microengineering* **2007**, *17* 781.

[40] K. Oldham, J. Pulskamp, R. Polcawich, P. Ranade, M. Debey, *Integrated Ferroelectrics* **2007**, *95* 54.

Author Manuscript

This article is protected by copyright. All rights reserved.

[41] M. Tani, M. Akamatsu, Y. Yasuda, H. Toshiyoshi, In *2007 IEEE 20th International Conference on Micro Electro Mechanical Systems (MEMS), 21-25 Jan, 2007, Hyogo Japan*, 9827272. **2007** .

[42] D. Dezest, O. Thomas, F. Mathieu, L. Mazenq, C. Soyer, J. Costecalde, D. Remiens, J. F. Deu, L. Nicu, *J. Micromech. Microeng.* **2015**, *25*, 035002.

[43] A. Milojević, M. Shin, K. R. Oldham, *Journal of Intelligent Material Systems and Structures* **2021**, *33* 136.

[44] Y. Zhu, E. T. Filipov, *International Journal of Mechanical Sciences* **2021**, *202-203*, 106537.

[45] N. Chronis, L. P. Lee, *Journal of Microelectromechanical Systems* **2005**, *14*, 4 857.

[46] I. H. Grinberg, N. Maccabi, A. Kassie, D. Elata, *Journal of Microelectromechanical Systems* **2017**, *26* 1279.

[47] W. Dai, K. Lian, W. Wang, *Microsyst. Technol.* **2005**, *11* 526.

[48] S. Timoshenko, *J.O.S.A. & R.S.I.* **1925**, *11*.

[49] A. Dick, *Journal of Mechanical Engineerign* **2013**, *59* 50.

Author Manuscript

This article is protected by copyright. All rights reserved.

Yi Zhu is a Post Doctoral Researcher in the Mechanical Engineering Department at the University of Michigan, Ann Arbor. Yi holds a Ph.D. Degree in Civil Engineering and Scienti□c Computing from the University of Michigan. Previously, Yi received his Master degree at University of California at Berkeley, and his Bachelor degree at Tongji University, Shanghai, China. His research focuses on developing analytical tools and fabrication methods for building origami-inspired active structures across all length scale. Learn more about his research at his personal website: https://sites.google.com/view/yi-zhu

Anan Ghrayeb is a Ph.D. candidate in Mechanical Engineering at the University of Michigan, Ann Arbor, MI, USA. Anan received a B.S. degree in Mechanical Engineering from the University of Illinois at Urbana-Champaign. His current research focuses on the design and scalability of origami-inspired microsystems, speci□cally for application in testing of biological matter. He is especially interested in further investigating force dynamics of the tumor microenvironment, whose data can be used to develop therapeutics for cancer.

Joonyoung Yu is a PhD candidate in the Department of Mechanical Engineering at the University of Michigan, Ann Arbor, MI, USA. Previously, he received a Master's degree in Mechanical Engineering from his current institution and a bachelor's degree in Mechanical Engineering from Purdue University, West Lafayette, IN, USA. His research focuses on PZT MEMS mirrors and biomedical imaging systems for early cancer detection and brain imaging.

Yiwei Yang is a PhD candidate in Mechanical Engineering at the University of Michigan, Ann Arbor, MI, USA. Yiwei received a Master's degree in Mechanical Engineering from the University of Michigan. Previously, Yiwei received his Bachelor degree both at University of Michigan and Shanghai Jiao Tong University, Shanghai, China. His research focuses on modeling and control in micro-robotics systems. Yiwei speci□cally focuses on dynamic, nonlinear modeling and control techniques of thin-□lm PZT/ET MEMS actuators used in micro-origami or micro-mirror systems.

Evgueni T. Filipov is an Associate Professor in the Departments of Civil and Environmental Engineering, and Mechanical Engineering at the University of Michigan, Ann Arbor. His research interests are focused on the underlying mechanics of origami-inspired deployable and recon□gurable structures. These mechanics are employed to improve sti□ness, functionality, and manufacturing of the folded systems. He holds M.S. and Ph.D. degrees in Civil Engineering from the University of Illinois at Urbana-Champaign, and a B.S. from Rensselaer Polytechnic Institute. He has received the ASCE EMI Leonardo da Vinci Award (2023), the NSF CAREER Award (2020), the DARPA Young Faculty Award (2018), the Cozzarelli Prize from the National Academy of Sciences (2015), and the NSF Graduate Research Fellowship. Learn more about his research at his lab's website: http://drsl.engin.umich.edu/

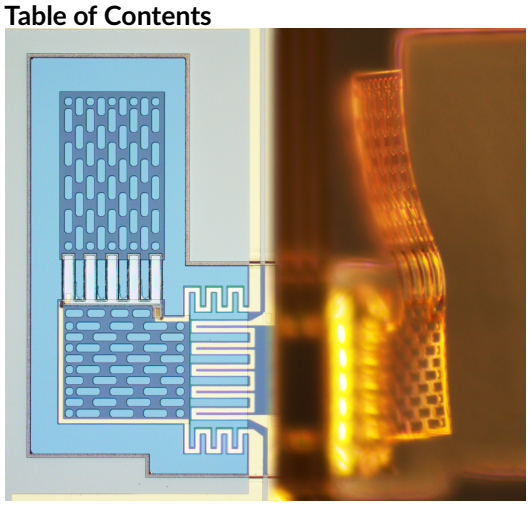
Kenn R. Oldham is a Professor in the Department of Mechanical Engineering at the University of Michigan, Ann Arbor. He received a B.S. degree in Mechanical Engineering from Carnegie Mellon University and a Ph.D. degree in Mechanical Engineering from the University of California at Berkeley. His research focuses on the intersection of control systems and micro-scale sensing and actuation, with interests in design for controllability, optimal and robust control, estimation and identi□cation for microsystems, and novel sensor and actuator design. Applications include micro-robotics, miniature imaging tools, and inertial and physiological sensing. He is a recipient of the NSF CAREER Award and DARPA Young Faculty Award, and an Associate Director of the Weil Institute for Critical Care Research and Innovation at the University of Michigan.

Author Manuscript

This article is protected by copyright. All rights reserved.

Author Manuscript

Table of Contents



This work creates mixed-transducer micro-origami systems that harness the advantages of lead zirconate titanate (PZT) transducers together with polymer based electro-thermal transducers to achieve manipulation and sensing at the micro-scale. The versatile fabrication approach and the demonstrated micro-origami systems could be used for applications in active metamaterials, micro-robots, surgical tools, biomedical sensing, and much more.

This article is protected by copyright. All rights reserved.